

1
2
3
4
5
6
7
8
9
10
11
12
13
14
15
16
17
18
19
20
21

Solid-state NMR characterization of triacylglycerol and polysaccharides in coffee beans

Noriko Kanai¹, Naoki Yoshihara², Izuru Kawamura^{1, *}

1. Department of Chemistry, Chemical Engineering, and Life Science, College of Engineering Science, Yokohama National University
2. Instrumental Analysis Center, Yokohama National University.

* Corresponding author; izuruk@ynu.ac.jp

22 **Abstract**

23 It is important to understand the structural characteristics of triacylglycerol (TAG),
24 polysaccharides and trace elements in coffee beans, so that residues can be reutilized in
25 applications including biodiesel oils. Here, we performed ^1H and ^{13}C solid-state NMR
26 measurements on Indonesian green beans, roasted beans, and spent coffee grounds
27 (SCGs). In the NMR spectra, there were liquid-like TAG containing linoleic acids based
28 on observed signals of $-\text{CH}=\text{CH}-\text{CH}_2-\text{CH}=\text{CH}-$ group in an acyl chain, which play a role
29 in decreasing TAG's melting point. We have found TAG was still abundant in the SCGs
30 from NMR spectra. After lipids were removed from SCGs, the intensity of the TAG signal
31 decreased considerably, with approximately 64% of the TAG was successfully extracted.
32 We described the chemical structure of TAG in coffee beans and demonstrated that it is
33 possible quantify the amount of extracted TAG using solid-state NMR.

34

35 **Introduction**

36 Coffee is one of the world's most popular beverages, and more than 400 billion cups
37 of coffee are consumed each year [1]. Approximately 9.5 million tons of coffee beans
38 were consumed in 2017, and this is increasing year by year [2]. Approximately 8 million
39 tons of spent coffee grounds (SCGs) are generated annually [3]. They are now classified
40 as food industry waste, and there is a responsibility to establish an efficient and
41 comprehensive method for reusing or adding value to SCGs. Research on SCGs has
42 sharply increased in the past ten years [1]. SCGs can be reused to produce fuel for
43 industrial boilers, as a substrate for the cultivation of microorganisms, and as a raw
44 material to produce ethanol, among other uses [4]. Biodiesel is a source of renewable
45 energy, and the production of biodiesel has been dramatically increased in past ten years.
46 According to some reports, oils from SCGs have the potential to be used in biodiesel oil
47 [5-7]. Furthermore, coffee beans contain polysaccharides in their cell walls such as
48 cellulose and hemicellulose. [3,6,8]. The extracts from coffee oils, including SCGs, have
49 not been completely characterized at the molecular level, which is important SCGs can
50 be used for green chemistry applications.

51 Coffee beans contain a complex mixture of hundreds of different compounds. Lipids
52 are abundant in coffee beans and SCGs [3,8,9]. Lipids still represent about 10 to 20 % of
53 the mass of SCGs [1,10,11]. The major lipid in coffee beans is triacylglycerol (TAG)
54 [10,12], which is widely found in animal fat and vegetable oil. TAG consists of three acyl
55 chains with saturated and unsaturated fatty acids. The unsaturated fatty acids are oleic
56 (18:1(n-9)), linoleic (18:2(n-6)) and linolenic (18:3(n-3)) acids [10].

57 Nuclear magnetic resonance (NMR) is an effective and non-destructive analytical tool
58 to identify the structure and dynamics of molecules [13–15]. Solution NMR analysis of
59 the extracts of roasted coffee beans (RCBs) and green coffee beans (GCBs) has been used
60 to analyze the structure of organic compounds and investigate their metabolomics to
61 classify beans from different geographic regions [16,17]. Solid-state NMR
62 characterization is a direct method for analyzing insoluble biomacromolecules, such as
63 polysaccharides in plant cell walls, membrane proteins, and amyloid peptides [18–22].
64 Additionally, the use of solid-state NMR with magic angle spinning (MAS) does not
65 require any complex sample treatment. If we could reveal detailed structural information
66 about the lipids in coffee beans via solid-state NMR analysis, we could estimate their
67 amounts and the degree of unsaturation in lipid molecules without needing to extract from

68 coffee beans. This would lead to a deeper understanding of how lipids extracted from
69 SCGs can be used as raw materials to generate biodiesel oil. Therefore, we investigated
70 the structures of TAG and polysaccharides from GCBs, RCBs and SCGs using ^1H and
71 ^{13}C solid-state MAS NMR techniques.

72

73 **Materials and Methods**

74 *Sample preparation*

75 The GCBs and RCBs were commercially available *Robusta* coffee varieties in Indonesia
76 that had been washed. GCBs and RCBs were ground using an electric coffee grinder
77 (Kalita, EG-45) for 70 s and for 40 s respectively, to a uniform particle size. Then hot
78 water was added to ground RCBs. Wet-ground RCBs were thinly spread on filter paper
79 and completely dried at room temperature at least 1 day. Completely dried ground RCBs
80 were called as SCGs. For the proton/deuterium exchange experiment, 450 mg of RCBs
81 was suspended in 5 mL of 99.5% D_2O (CIL) and then the RCBs were dried at room
82 temperature. TAG containing only oleic fatty acids in acyl chains ($\geq 97\%$, Sigma
83 Aldrich) was used as a reference sample.

84

85 *SEM*

86 The internal structures of the GCBs and RCBs were observed with field emission
87 scanning electron microscope (FE-SEM) (HITACHI, SU8010). GCBs were rapidly
88 freeze-dried and polished by embedding in a resin block to expose the section. RCBs
89 were divided into a several mm-sized pieces using a cutter and then were lyophilized by
90 a freeze-dryer (EYELA, FDU-2100).

91

92 *Extracting lipids from SCGs*

93 The equivalent of a cup of coffee SCGs, 10 g was gently stirred in 100 mL of *n*-hexane
94 at room temperature for 1 day. The solvent was removed by reduced pressure evaporation
95 at 80°C (EYELA, SB-1200). Approximately about 70 μl of lipids were extracted as a
96 clear yellow brown oil in liquid form, and solid residues were filtered (Figure 1). The
97 extraction rate of TAG was estimated by comparing integrated intensity ratio of the signal
98 at 2.6~2.7 ppm in ^1H -MAS NMR spectra. (Figure 3 (b) and Figure 4 (b))

99

100 *^1H and ^{13}C solid-state NMR experiments*

101 The GCBs, RCBs, SCGs samples as well as the solid residue and liquid lipids extracted
102 from the SCGs were directly packed into a 4.0 mm outer diameter zirconia NMR rotor.
103 ^1H -MAS, ^{13}C cross polarization-magic angle spinning (CP-MAS) and ^{13}C dipolar
104 decoupling-magic angle spinning (DD-MAS) solid-state NMR spectra were recorded at
105 room temperature with a recycle delay time of 4 s on a 600 MHz spectrometer (Bruker
106 Avance III) equipped with a 4.0 mm E-free MAS probe. The MAS frequencies were at
107 12.0 and 10.0 kHz for the ^1H and ^{13}C NMR experiments, respectively. The DD-MAS
108 method primarily detects ^{13}C NMR signals from the mobile components based on their
109 spin-lattice relaxation times compared with the recycle delay times [21, 22]. ^1H and ^{13}C
110 chemical shifts were referenced to tetramethylsilane at 0.0 ppm, respectively (Figure 1).

111

112 **Results and Discussion**

113 *SEM observations*

114 The cell walls in the GCBs and RCBs had strong honeycomb structures with pore sizes
115 of several tens of μm as shown in Figure 2. The honeycomb structure in the SEM image
116 of GCB is partly distorted because of the removal of moisture during lyophilization.
117 However, a similar honeycomb structure of the cell walls is evident in the GCB when
118 observed with an optical microscope (Supporting Information Figure S1). The pores of
119 the GCB and RCB are filled with liquid lipids, and the moisture, which was present in
120 the GCB but not in the RCB, was believed to be absorbed into the cell walls (see NMR
121 section below).

122

123 *Solid-state NMR characterization of TAG*

124 Firstly, we observed ^1H and ^{13}C solid-state NMR spectra of GCBs, RCBs and SCGs as
125 shown in Figure 3. In general, ^1H MAS NMR signals of a solid-state sample are quite
126 broad due to large huge ^1H - ^1H homonuclear dipolar interactions [21]. However, all three
127 ^1H MAS NMR spectra of GCBs, RCBs and SCGs had similar narrow spectral patterns,
128 except there was a broad signal at around 4.5 ppm in the GCBs (Figure 3 (a) to (c)).

129 We confirmed that the three fatty acids in the TAG molecule were a mixture of oleic,
130 and linoleic acids. The ^1H NMR peaks in all three spectra corresponded to A-J of TAG in
131 Figure 3 and complete assignments of ^1H NMR signals corresponding to A-J were
132 summarized in Supporting Information Table S2. The **F** signal (2.6 ppm) in all three
133 spectra belongs to protons directly bonded with the carbon sandwiched between two –

134 C=C– bonds as -CH=CH-CH₂-CH=CH- in linoleic acid. Most –C=C– bonds in natural
135 unsaturated fatty acids have a *cis*-conformation, which causes a bend in the alkyl chain
136 and molecules that are not well stacked. TAG is likely a liquid in coffee beans at room
137 temperature because of the –C=C– bonds in the unsaturated fatty acids. All the peaks
138 assigned to TAG in the ¹H MAS NMR observations were remarkably sharp despite the
139 use of natural products without any pretreatment. It appears that the amount of
140 unsaturated fatty acids in coffee beans is higher than the amount of saturated fatty acids.
141 The scale of the SCGs spectrum in Figure 3 (Left) was enlarged five times because the
142 intensity was smaller than that of the GCBs and RCBs. This indicates that some TAG was
143 extracted during coffee brewing, decreasing the amount of TAG in the SCGs compared
144 to the same volume of RCBs. There was a broad signal at approximately 4.5 ppm in the
145 GCBs due to fixed moisture, which accounts for approximately 5 to 10% of the dry weight
146 [23,24]. The broadness of this signal is likely due to the slow mobility of water molecules
147 absorbed into cell walls. The moisture content of coffee beans is sharply reduced during
148 the roasting process; consequently, signals derived from water in cell walls were not
149 appeared at around 4.5 ppm in the ¹H NMR of RCBs (Figure 3 (b)) or SCGs (Figure 3(c)).

150 The ¹³C DD-MAS NMR spectra of the GCBs, RCBs and SCGs revealed similar
151 patterns of chemical shifts (Figure 3 right). All the sharp peaks, except the broad peak of
152 **K** (60~63 ppm) and **L** (70~77 ppm), could be assigned to TAG, with the -C=C- double
153 bond of linoleic acids at around 130 ppm (Supporting information Table S2). **K** and **L** are
154 derived from the polysaccharides that constitute cell walls in coffee beans. Components
155 of the cell wall have restricted their molecular mobility due to high crystallization, so **K**
156 and **L** are not as sharp as the peaks assigned to TAG.

157 After extracting the lipids from the SCGs, the liquid lipids and the solid residues
158 were analyzed by ¹H MAS NMR and ¹³C DD-MAS NMR (Figure 4). The sharpness of
159 the peaks in Figure 4 (a) and (c) suggest a high purity and consistent quality in the
160 extracted TAG from the SCGs. A single peak appeared at 172.3 ppm in (c) indicates the
161 absence of free fatty acids and that is a great advantage for transesterification process of
162 biodiesel production in general [25]. These results are also consistent with chemical shifts
163 of commercial TAG, whose fatty acids are only oleic acids (Supporting Information
164 Figure S2). The broad peak around 4 ppm in Figure 4 (b) may be due to water added to
165 the brewing process or adsorbed water during the drying process. The peak at 110 ppm
166 (Figure 4 (c)) is from the Teflon coating spacer used to avoid spillage of liquid lipids in

167 the zirconia NMR rotor during the acquisition. The signals marked with an asterisk (*) in
168 Figure 4 (d) are likely the polysaccharides that constitute the cell walls of coffee beans,
169 which indicates that the cell walls were not destroyed during the hexane treatment. On
170 the other hand, the ^{13}C NMR signals of TAG in the dried residue (Figure 4 (d)) were
171 relatively low compared to those of the RCBs and SCGs (Figure 3), suggesting that the
172 TAGs were mostly extracted by the hexane treatments, but a small amount of TAG
173 remained. The sharpness of the peaks in ^1H MAS NMR and ^{13}C DD-MAS NMR spectra
174 (Figure 4 (a) and 4 (c)) indicated the uniformity of extracted lipids from SCGs, and a high
175 level of similarity with the commercial triacylglycerol sample (Supporting Figure S3 and
176 Table S2) demonstrated the high purity of the TAG. Different from soybean oil, palm oil
177 and cottonseed oil which are typical vegetable oils generated biodiesel fuel [26], SCGs
178 does not need newly cultivated lands nor completely compete with food. From our NMR
179 results, SCGs are promising raw materials for generating biodiesel fuel. However, TAG
180 seems to remain in the residues after delipidization process (Figure 4 (a) and 4 (c)), so an
181 improvement extraction rate of TAG would be future issues. In addition, solid-state ^1H
182 MAS NMR technology is also useful in the field of food science, as it is possible to
183 evaluate the quality of TAG rapidly.

184

185 *Solid-state NMR characterization of polysaccharides*

186 The spectra from ^{13}C CP-MAS NMR show the main components of the cell walls (Figure
187 5). Cellulose and hemicellulose are polysaccharides that constitute the primary cell wall.
188 There were high intensity peaks between 60 and 110 ppm representing carbons, constitute
189 the five- or six-membered rings of polysaccharides. Galactomannan, arabinogalactan and
190 cellulose are the most common polysaccharides in the coffee beans [8]. Using
191 SPINASSIGN based on the RIKEN ^1H and ^{13}C chemical shift database of metabolites,
192 the ^{13}C NMR signals at 81 and 102 ppm could be assigned to the galactose group of
193 polysaccharides [27]. This indicates signals at 81 and 102 ppm are from polysaccharides
194 included in hemicellulose. The broad signals of E, F and G are likely TAG and
195 glycoprotein sidechains [28], lignin aromatic carbons [28, 29] and the carbonyl groups of
196 lignin, hemicelluloses and the protein backbone [30]. The spectral similarities of the
197 GCBs, RCBs, SCGs and solid residues indicates that the cell wall structure was
198 maintained through the roasting, grinding, and delipidization processes. The presence of
199 strong intramolecular and intermolecular hydrogen bonds in cellulose microfibrils and

200 hemicellulose may explain the stable structure of the cell walls [8, 31]. Deuterium
201 secondary isotope shifts on ^{13}C NMR signals can be used to identify exchangeable
202 hydroxyl protons [32]. A comparison of the ^{13}C CP-MAS NMR spectra of RCBs and
203 D_2O -suspended RCBs revealed that the C6 signal of the suspended RCBs shifted partly
204 toward a higher field shift of 1 ppm (at 61.8 ppm) (Supporting Information Figure S3).
205 This suggests that water molecules can be reached easily at the cell walls and that they
206 dynamically interact with polysaccharides via hydrogen bonds. Cellulose can become an
207 attractive source of cellulose nanofibers oxidized by water-soluble 2,2,6,6-
208 tetramethylpiperidine-1-oxyl (TEMPO), which is a promising new functional material
209 [33]. The production of cellulose nanofibers from coffee bean will be our next focus.

210

211 **Conclusions**

212 Thick cell walls in the GCBs and RCBs were observed to form honeycomb structures
213 even after grinding or brewing, and lipids were contained in pores. ^1H and ^{13}C solid-state
214 NMR measurements have been performed to characterize the lipids and polysaccharides
215 in coffee beans that had not been processed, those that had been roasted, those that were
216 left over from coffee brewing, and those that had undergone lipid extraction. The structure
217 of lipids in coffee beans was determined by NMR analysis. TAG have mixture of oleic
218 and linoleic fatty acids, and they were successfully isolated in liquid form via
219 delipidization process. Structure of major polysaccharides as galactomannan,
220 arabinogalactan and cellulose in the coffee beans were characterized by ^{13}C solid-state
221 NMR. These characterizations will help advance research on generating biodiesel fuel
222 from the TAG.

223

224 **Acknowledgements**

225 This work was financially supported by ROUTE (Research Opportunity for
226 Undergraduates) program from Yokohama National University to N. K. and Yokohama
227 Academic Foundation (674) to I. K. The authors thank Prof. Kazuhiko Nishitani at
228 Tohoku University for his helpful advice about the SEM observation of the cell walls.
229 The authors also thank Mr. Shinji Ishihara at Instrumental Analysis Center of Yokohama
230 National University for his technical assistance with the optimization of NMR
231 spectrometer and probe performance. The authors wish to thank Prof. Akira Naito at
232 Yokohama National University for valuable discussions.

233

234 **Disclosure statement**

235 No potential conflict of interest is reported by the authors.

236

237

238 **References**

- 239 [1] Obruca S, Benesova P, Kucera D, et al. Biotechnological conversion of spent coffee
240 grounds into polyhydroxyalkanoates and carotenoids. *N. Biotechnol.* 2015;**32**:569–
241 574.
- 242 [2] Statistics data on International Coffee Organization “World coffee consumption”
243 (2018) <http://www.ico.org/>
- 244 [3] Jenkins RW, Ellis EH, Lewis EJ, et al. Production of biodiesel from Vietnamese waste
245 coffee beans: biofuel yield, saturation and stability are all elevated compared with
246 conventional coffee biodiesel. *Waste Biomass Valori.* 2017;**8**:1237–1245.
- 247 [4] Ballesteros LF, Teixeira JA, Mussatto SI. Chemical, functional, and structural
248 properties of spent coffee grounds and coffee silverskin. *Food Bioprocess Tech.*
249 2014;**7**:3493–3503.
- 250 [5] Campos-Vega R, Loarca-Piña G, Vergara-Castañeda HA, Oomah BD. Spent coffee
251 grounds: A review on current research and future prospects. *Trends Food Sci Tech.*
252 2015;**45**:24–36.
- 253 [6] Kovalcik A, Obruca S, Marova I. Valorization of spent coffee grounds: A review.
254 *Food Bioprod Process.* 2018;**110**:104–119.
- 255 [7] Kookos IK. Technoeconomic and environmental assessment of a process for biodiesel
256 production from spent coffee grounds (SCGs). *Resour Conserv Recy.*
257 2018;**134**:156–164.
- 258 [8] Arya M, Rao LJM. An impression of coffee carbohydrates. *Crit Rev Food Sci Nut.*
259 2007;**47**:51–67.
- 260 [9] Janissen B, Huynh T. Chemical composition and value-adding applications of coffee
261 industry byproducts: A review. *Resour Conserv Recy.* 2018;**128**:110–117.
- 262 [10] Toci AT, Neto VJMF, Torres AG, Farah A. Changes in triacylglycerols and free fatty
263 acids composition during storage of roasted coffee. *LWT - Food Sci. Technol.*
264 2013;**50**:581–590.
- 265 [11] D’Amelio N, De Angelis E, Navarini L, et al. Green coffee oil analysis by high-

- 266 resolution nuclear magnetic resonance spectroscopy. *Talanta* 2013;**110**:118–127.
- 267 [12] Jham GN, Nikolova-Damyavova B, Viera M, et al. Determination of the
268 triacylglycerol composition of coffee beans by reverse-phase high-performance
269 liquid chromatography. *Phytochem Anal.* 2003;**14**:310–314.
- 270 [13] Ramakrishnan V, Luthria DL. Recent applications of NMR in food and dietary
271 studies. *J Sci Food Agric.* 2017;**97**:33–42.
- 272 [14] Kasai M, Lewis AR, Ayabe S, et al. Quantitative NMR imaging study of the cooking
273 of Japonica and Indica rice. *Food Res Int.* 2007;**40**:1020–1029.
- 274 [15] Teramura H, Sasaki K, Kawaguchi H, et al. Differences in glucose yield of
275 residues from among varieties of rice, wheat and sorghum after dilute acid
276 pretreatment, *Biosci Biotechnol Biochem.* 2017;**81**:1650–1656.
- 277 [16] Wei F, Furihata K, Koda M, et al. ¹³C NMR-based metabolomics for the
278 classification of green coffee beans according to variety and origin. *J Agric Food*
279 *Chem.* 2012;**60**:10118–10125.
- 280 [17] Wei F, Furihata K, Hu F, et al. Complex mixture analysis of organic compounds in
281 green coffee bean extract by two-dimensional NMR spectroscopy. *Magn Reson*
282 *Chem.* 2010;**48**:857–865.
- 283 [18] Komatsu T, Kikuchi J. Comprehensive signal assignment of ¹³C-labeled
284 lignocellulose using multidimensional solution NMR and ¹³C chemical shift
285 comparison with solid-state NMR. *Anal Chem.* 2013;**85**:8857–8865.
- 286 [19] Phyto P, Wang T, Yang Y, et al. Direct determination of hydroxymethyl
287 conformations of plant cell wall cellulose using ¹H polarization transfer solid-state
288 NMR. *Biomacromolecules*, 2018;**19**:1485–1497.
- 289 [20] Kono H. Characterization and properties of carboxymethyl cellulose hydrogels
290 crosslinked by polyethylene glycerol. *Carbohydr Polym.* 2014. **106**, 84–93.
- 291 [21] Naito A, Kawamura I, Javkhlantugs N. Recent solid-state NMR studies of membrane
292 proteins. *Annu Rep NMR Spectroscop.* (Edited by Graham A. Webb, Elsevier).
293 2015; **86**:Chap. 5;333–411.
- 294 [22] Naito A, Matsumori N, Ramamoorthy A. Dynamic membrane interactions of
295 antibacterial and antifungal biomolecules, and amyloid peptides, revealed by solid-
296 state NMR spectroscopy. *BBA Gen Subjects.* 2018; **1862**:307–323.
- 297 [23] Pittia P, Nicoli MC, Sacchetti G. Effect of moisture and water activity on textural
298 properties of raw and roasted coffee beans. *J Texture Stud.* 2007;**38**:116–134.

- 299 [24] Ramalakshmi K, Kubra IR, et al. Physicochemical characteristics of green coffee:
300 Comparison of graded and defective beans. *J Food Sci.* 2007;**72**:333-337.
- 301 [25] Al-Hamamre Z, Foerster S, Hartmann F, Kröger M, Kaltschmitt M. Oil extracted
302 from spent coffee grounds as a renewable source for fatty acid methyl ester
303 manufacturing. *Fuel.* 2012;**96**:70-76.
- 304 [26] Issariyakul T, Dalai AK. Biodiesel from vegetable oils. *Renew Sustain Energy Rev.*
305 2014;**31**:446-471.
- 306 [27] Chikayama E, Sekiyama Y, Okamoto M, et al. Statistical indices for simultaneous
307 large-scale metabolite detections for a single NMR spectrum. *Anal Chem.*
308 2010;**82**:1653–1658.
- 309 [28] Dick-Pérez M, Zhang Y, Hayes J, et al. Structure and interactions of plant cell-wall
310 polysaccharides by two- and three-dimensional magic-angle-spinning solid-state
311 NMR. *Biochemistry* 2011;**50**:989–1000.
- 312 [29] Gilardi G, Abis L, Cass AEG. Carbon-13 CP/MAS solid-state NMR and FT-IR
313 spectroscopy of wood cell wall biodegradation. *Enzyme Microb Technol.*
314 1995;**17**:268–275.
- 315 [30] Reddy KO, Ashok B, Reddy KRN, et al. Extraction and characterization of novel
316 lignocellulosic fibers from *Thespesia lampas* Plant. *Int J Polym Anal Charact.*
317 2014;**19**:48–61.
- 318 [31] Nishitani, K. Construction and restructuring of the cellulose-xyloglucan framework
319 in the apoplast as mediated by the xyloglucan-related protein family-A
320 hypothetical scheme. *J. Plant Res.* 1998, **111**: 159-166.
- 321 [32] Hanashima, S, Kato K, Yamaguchi, Y. ¹³C-NMR quantification of proton exchange
322 at LewisX hydroxyl groups in water. *Chem. Commun.* 2011, **47**: 10800-10802.
- 323 [33] Saito T, Kimura S, Nishiyama Y, Isogai A. Cellulose Nanofibers Prepared by
324 TEMPO-Mediated Oxidation of Native Cellulose. *Biomacromolecules.*
325 2007;**8**:2485–2491.

326
327
328
329
330

331

332

333

334

335

336 **Figure Captions**

337 Figure 1. The experimental design of solid-state MAS NMR characterization in coffee
338 beans [green coffee beans (GCBs); roasted coffee beans (RCBs); spent coffee grounds
339 (SCGs)] and solid residue and liquid lipids extracted from SCGs.

340

341 Figure 2. SEM images of cell walls in (a) GCBs and (b) RCBs.

342

343 Figure 3. [Left] ^1H MAS NMR spectra of (a) GCBs, (b) RCBs and (c) SCGs (scale
344 magnified five times), with letters from A to J indicating peaks that correspond to
345 structures in two fatty acids (oleic, and linoleic acid); and [Right] ^{13}C DD-MAS NMR
346 spectra of (d) GCBs, (e) RCBs, and (f) SCGs, with letters K and L indicating
347 polysaccharides. For the ^1H MAS NMR, all three spectra were accumulated from 200
348 scans and each experimental time is 7 minutes. For the ^{13}C DD-MAS NMR, all three
349 spectra were accumulated from 13,000 scans and each experimental time is around 11
350 hours.

351

352 Figure 4. [Left] Spectra from ^1H MAS NMR of (a) extracted liquid TAG and (b) solid
353 coffee residues after hexane treatment (Number of scans = 200, total experimental time
354 = 4 min 6 sec.), and [Right] spectra from ^{13}C DD-MAS NMR of (c) extracted liquid TAG
355 (Number of scans = 600, total experimental time = 30 min 33 sec.) and (d) solid coffee
356 residues after hexane treatment (Number of scans = 13000, total experimental time = 11
357 h 1 min 6 sec.).

358 .

359

360 Figure 5 [Inset] Structure of cellulose; and spectra from ^{13}C CP-MAS NMR of (a) GCBs,
361 (b) RCBs, (c) SCGs, and (d) solid coffee residues after hexane treatment (Number of
362 scans = 5000, total experimental time = 4 h 14 min 43 sec.).

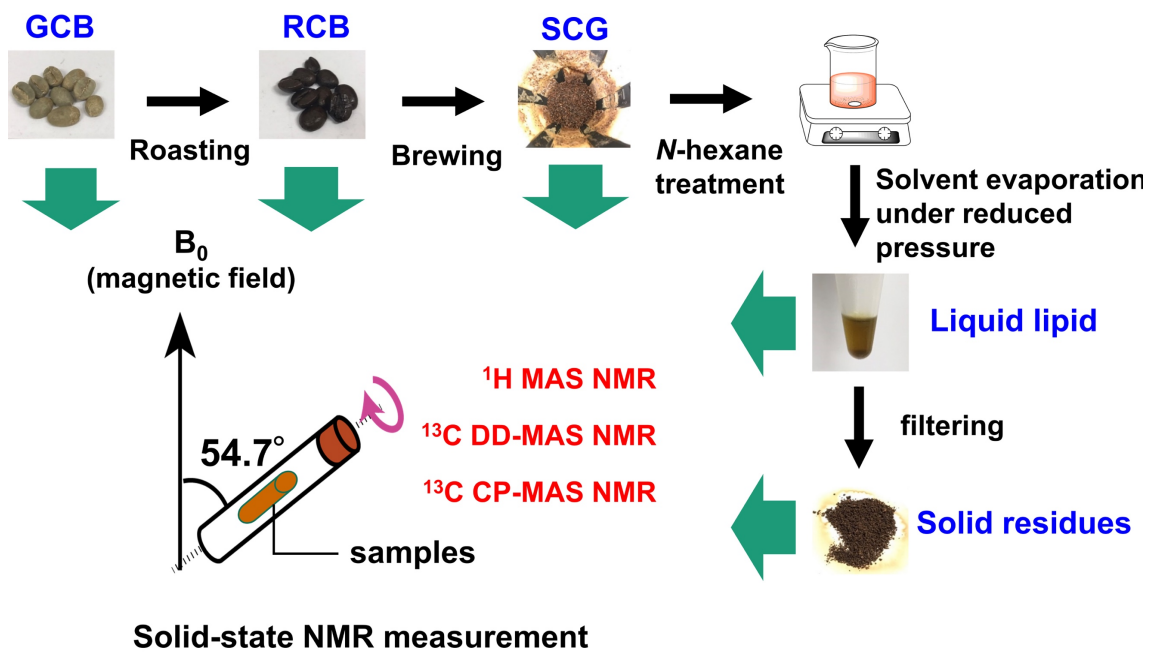


Figure 1
N. Kanai et al. (2018)

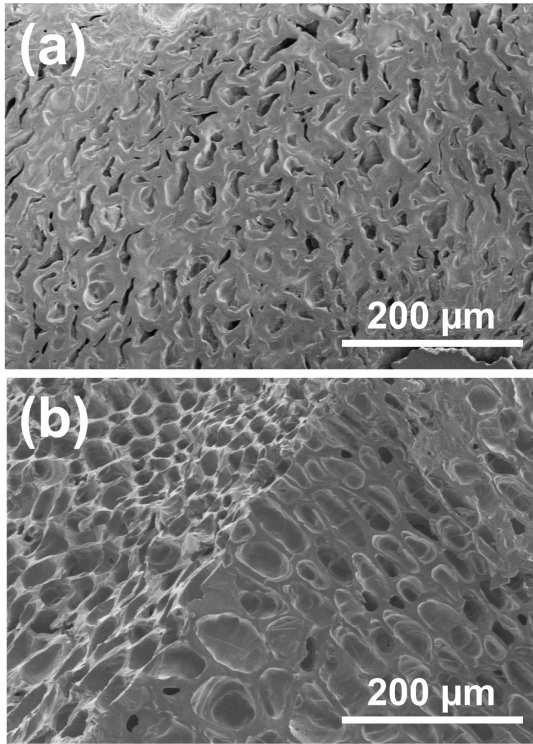


Figure 2
N. Kanai et al. (2018)

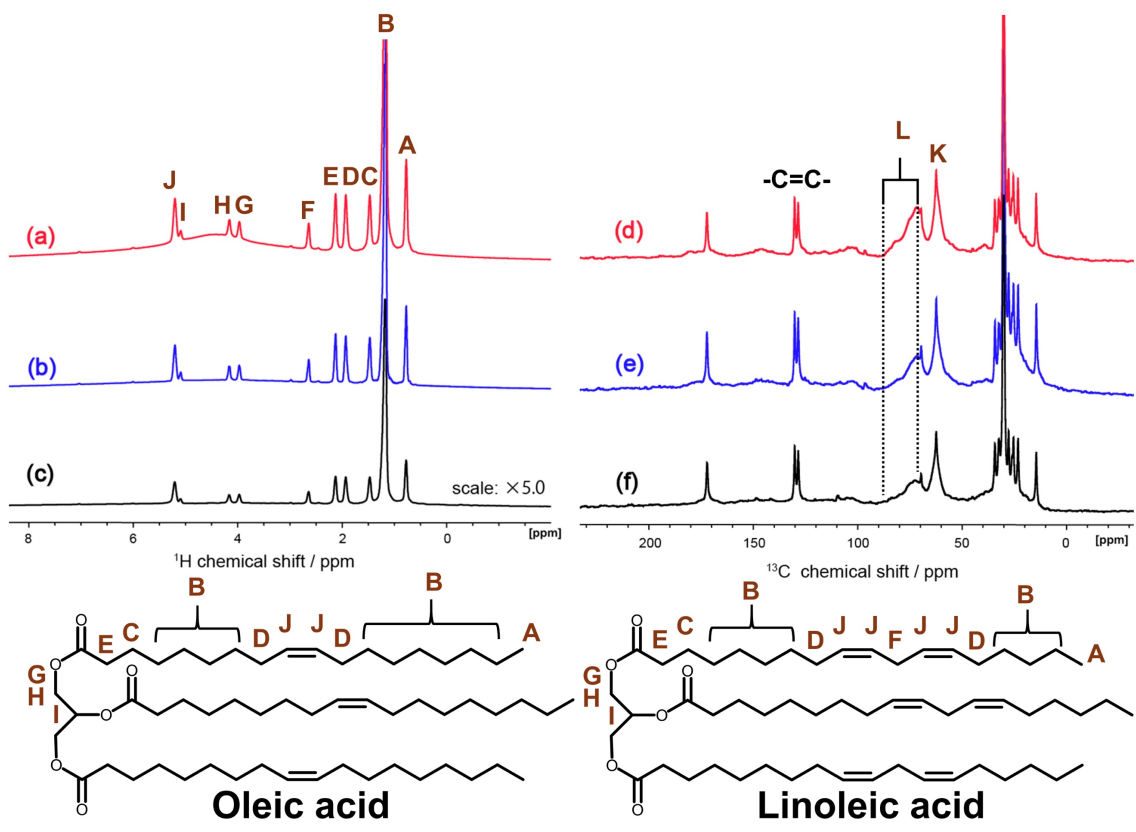


Figure 3 N. Kanai et al. (2018)

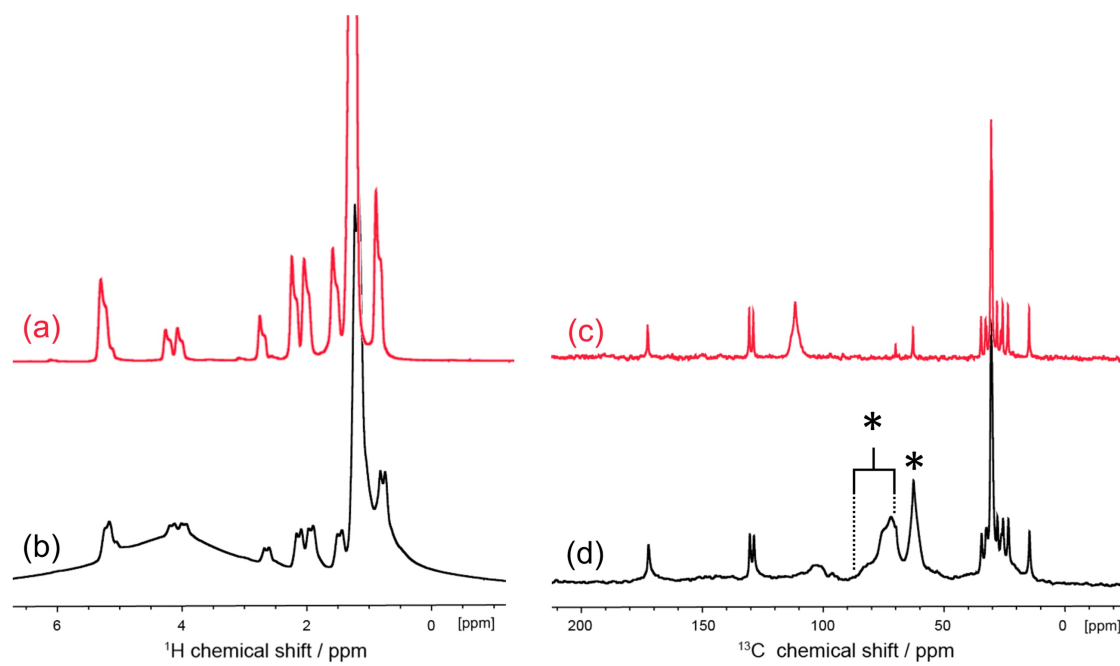


Figure 4
N. Kanai et al. (2018)

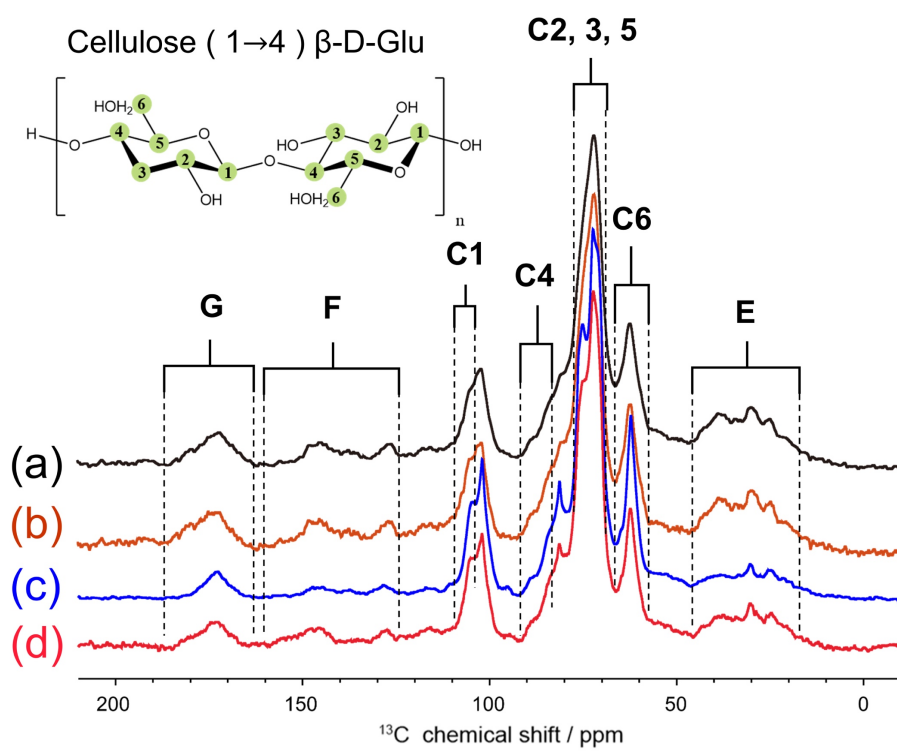


Figure 5
N. Kanai et al. (2018)